Pressure steam ageing of silica filled silicone rubber : Degradation mechanisms

Manar Ramram, Lénaïk Belec, Jean-François Chailan, François Perseil Rouillard, François-Xavier Perrin

Polymer Degradation and Stability 237 (2025) 111332

Contents lists available at ScienceDirect

Polymer Degradation and Stability

journal homepage: www.journals.elsevier.com/polymer-degradation-and-stability

Pressure steam ageing of silica filled silicone rubber : Degradation mechanisms

Manar Ramram [a,b], Lénaïk Belec [b], Jean-François Chailan [b], François Perseil Rouillard [a], François-Xavier Perrin [b,*]

[a] TECHNETICS GROUP, Saint-Etienne, France
[b] Université de Toulon, MAPIEM, Toulon, France

ARTICLE INFO

Keywords:
Silicone rubber
Silica
Polymer-filler interfaces
Steam
Hydrolysis

ABSTRACT

Silica filled silicone rubber compound was hydrothermally aged under a complex condition consisting of a succession of vacuum phases at 80 °C and exposure to pressure steam at 134 °C. The results from various physico-chemical analysis techniques indicate that hydrothermal ageing has significantly affected both the polymer network and the polymer-filler interfaces, allowing the identification of the primary degradation mechanisms. Solvent swelling and solid ^{29}Si CP-MAS NMR analysis evinced that hydrolytic scission reactions predominate in the early stages of ageing and are compensated by recombination reactions for the subsequent cycles.

The volatilization of cyclic oligomers, resulting from the backbiting reaction, led to polymer loss and an associated increase in silica content within the silicone rubber compound, as confirmed by FTIR and TGA analyses. Significant changes occurred at the polymer-filler interfaces during the first few hundred cycles, including the formation of covalent bonds at the silica surface, replacing the physical interactions. These findings were further supported by solid-state ^{29}Si CP-MAS NMR analysis and ammonia-modified swelling experiments.

1. Introduction

Since their commercialization in the early '40 s, silicone rubber materials have been steadily gaining ground in the high-performance applications market [1,2]. They owe their success to the combined intrinsic synergetic properties of inorganic Si-O siloxane bonds and the organic side groups, resulting in high mobility, enhanced thermal and chemical stability, excellent resistance to attack by ozone, oxygen and sunlight [3–5]. The mechanical properties of these materials are improved by the incorporation of nanometric fillers, mainly fumed [6,7] and precipitated silica [6,8,9], through polymer-filler and filler-filler interactions. However, the hydrolytic degradation of silicone rubber is of concern in some specific industrial applications. In fact, because siloxane bond Si—O is sterically unhindered and strongly polar, it is subject to heterolytic cleavage [10]. Hydrolysis of the siloxane bond, leading to two hydroxyl-terminated chains [11] can be followed by redistribution [12] or depolymerization process. The silanol groups formed during hydrolysis can also re-condense, depending on the proportion of water in the system. The effective activation energy of polydimethylsiloxane (PDMS) hydrolysis varies from 67 to 125 kJ/mol [11, 13,14] and the extent of the degradation depends on temperature, time and exposure medium (liquid water or steam)[11]. Metkin et al. [13] reported that the limiting temperature for hydrolytic stability of polyorganosiloxanes depends on their structure and the nature of lateral groups. For instance, when methyl groups are substituted with ethyl, fluoropropyl or phenyl groups, the limiting temperature for hydrolytic stability increases (e.g., 258 °C for polymethylphenylsiloxane vs 198 °C for polydimethylsiloxane). Hydrolytic stability thus increases with more bulky and hydrophobic substituent groups. On the other hand, the presence of impurities, such as the residues from tin octoate, the catalyst used in the cure of RTV (room temperature vulcanization) polysiloxanes, can seriously impair the hydrolytic stability of silicone rubber materials [15]. Acid and base species, even in small quantities, play an important role in catalyzing the hydrolysis reaction and lowering the onset temperature of silicone rubber degradation. The presence of 5 % KOH in PDMS leads to a spectacular reduction in the temperature at which PDMS begins to degrade under inert conditions, from 350 °C to 110 °C [16]. In the presence of strong acids or bases, the hydrolytic degradation has been reported to occur at temperatures as low as 25 °C [10] or 40 °C [17]. Ducom et al. [18] reported that degradation rates of PDMS fluids at 24 °C were higher in highly acidic (pH 2) and basic (pH 12) solutions than in demineralized water. A review of the literature reveals that the

* Corresponding author.

https://doi.org/10.1016/j.polymdegradstab.2025.111332
Received 21 November 2024; Received in revised form 6 March 2025; Accepted 16 March 2025
Available online 17 March 2025

work reported to date focuses on changes in the structure of the silicone matrix, without discussing the role played by silica fillers or polymer-filler interfaces in the evolution of the material's properties. Therefore, the aim of this study is to assess the degradation mechanisms of a crosslinked, silica filled, silicone rubber compound under the prion sterilization cycle, consisting of alternating vacuum and steam phases. Particular attention will be paid to rearrangements that occur at polymer-filler interfaces. Following on from this study, a forthcoming paper will be dedicated to the influence of the material degradation on its mechanical properties.

2. Materials and methods

2.1. Material processing and ageing

The silicone rubber compound studied in this work was composed of a high consistency silicone gum, amorphous silica reinforcing fillers (Fig. S1), processing aid and crosslinking agent. The silicone gum was a polyvinyldimethylsiloxane (VMQ) polymer, the number average molecular weight was about 300 000 g/mol. A hydroxyl terminated low molecular weight polydimethylsiloxane fluid was used as the processing aid. The supporting information provides detailed chemical structure of the VMQ polymer and the processing aid (Fig. S2).

The crosslinking agent was 2,4 bis dichlorobenzoyle, a non-vinyl specific peroxide. Sheets of 2 mm thickness were cured by compression molding at 110 °C, for 10 min, using a Mapelli 80T press at a pressure of 200 bar. Then, the sheets were post-cured in an air-circulating oven for 4 h at a temperature of 200 °C. The ageing was performed using a WH Lisa 17 sterilizer. A standard prion cycle was used, consisting of 3 vacuum draws at 80 °C, followed by exposure to dry saturated steam at 134 °C at an overpressure of 2.2 bars. The cycle ends with vacuum drying at 80 °C (Fig. 1).

5 sets of samples were aged in the sterilizer at 100, 200, 500, 1000 and 2000 standard ageing cycles. The aged samples were named AX, with X the corresponding number of ageing cycles, and P for pristine sample. Each set of samples consisted of 2 mm thickness sheets that were suspended in the sterilizer and aged without any mechanical stress. One set of samples was aged at a time to avoid repeated opening and closing of the sterilizer.

2.2. Characterization

2.2.1. Scanning electronic microscopy (SEM)

Surface of pristine and aged samples was observed using a Zeiss Supra 40 vp scanning electron microscope with a 6 keV beam. Samples were not cleaned and were directly analyzed after deposition of a thin layer of gold to minimize charging effects. Micrographs were taken using Inlens mode at magnifications of 200X and 2000X.

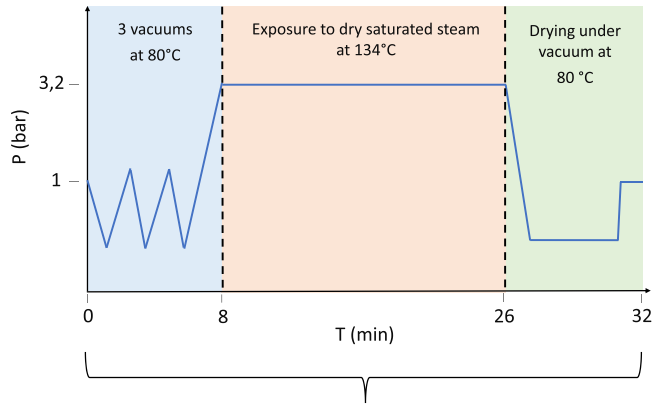

Fig. 1. Standard ageing cycle.

2.2.2. Weight loss

Silicone rubber sheets of 2 mm thickness were weighted before and after ageing using a ACCULAB / VICON scale with a measurement inaccuracy of ± 5 mg. The percentage weight loss was determined using Eq. (1):

$$\text{Weight loss}(\%) = 100 * \frac{w_i - w_f}{w_i} \quad (1)$$

Where and are respectively the weight before and after ageing.

2.2.3. Thermogravimetric analysis (TGA)

Thermogravimetric analyses were conducted on a Q600 SDT from TA Instruments. Around 10 mg of specimen, cut from the center of 2 mm silicone rubber sheets, were placed in an alumina pan and heated from room temperature to 850 °C at a rate of 10 °C/min, under nitrogen flow of 100 mL/min. Before each analysis, a purge was performed under nitrogen flow of 400 mL/min for 20 min, to drive away residual air molecules. The *temperature* at 5 % weight loss ($T_{d5\ \%}$) was identified as the *onset degradation temperature*.

2.2.4. Infrared spectroscopy

Fourier Transform Infrared Spectroscopy (FTIR) analyses of pristine and aged samples were performed on an IS50 spectrometer from THERMO NICOLET. The spectra were obtained using a diamond ATR crystal and recorded with a resolution of 8 cm^{-1} and an accumulation of 16 scans.

2.2.5. Equilibrium swelling

Two swelling protocols were conducted simultaneously to monitor the evolution of total and chemical crosslink density during ageing and to determine the contribution of physical polymer-filler interactions to the total crosslink density. Three swelling specimens were cut from the 2 mm thickness silicone rubber sheets using a die-cutter of 9 mm diameter, and the initial weight was determined for each specimen.

Protocol 1: swelling in methylcyclohexane

Each specimen was placed in a vial and 10 mL of methylcylohexane (Thermofisher, 99 %) were added and the vial was then sealed. The swelling was conducted for 7 days, at ambient temperature, until equilibrium. After 7 days, the specimen was removed from the vial and the solvent at specimen surface was quickly removed using an absorbing paper and then weighted to obtain the swollen weight. The specimens were then left under fume hood for 2 days to evaporate the absorbed solvent and weighted to determine the final weight.

Protocol 2: swelling in methylcyclohexane under ammonia atmosphere

Each specimen was placed in an open vial and 10 mL of methylcyclohexane were added. The open vials were then placed in a desiccator containing excess of concentrated ammonium hydroxide solution NH_4OH (28 - 30 % in water, Thermoscientific) and the desiccator was then sealed, which allows the formation of ammonia atmosphere. The ammonia is known for its capacity to break the hydrogen bonds between silanols groups at the surface of silica fillers and polymer chains (Fig. S3) [19] and thus, to determine contribution of physical polymer-filler interactions to the total crosslink density. As for the first protocol, the swelling was conducted for 7 days until equilibrium and the desiccator was not opened during the whole process. The swollen and final weight of the specimens were determined following the same process as for protocol 1.

For each protocol, the swelling ratio (SR) and the extractable fraction in the solvent (EF) were calculated using Eqs. (2) and (3), respectively [20]:

$$SR(\%) = \frac{w_f - (w_i * F_{\text{silica}}) + (w_s - w_f) * (\rho_e/\rho_s)}{w_f - (w_i * F_{\text{silica}})} * 100 \quad (2)$$

$$EF(\%) = \frac{w_i - w_f}{w_i * (1 - F_{\text{silica}})} * 100 \quad (3)$$

Where the initial weight of the specimen, the weight of the swollen specimen, the final weight of the specimen after evaporation of solvent, the weight fraction of silica fillers, = 0.97 g/cm^3 the density of the polymer [21] and = 0.77 g/cm^3 the density of the solvent: here, methylcyclohexane.

From swelling data determined for both protocols, parameter was calculated. The parameter, first introduced by Vondracek et al. [19] as the network chain decrement, is proportional to the fraction of total network resulting from physical polymer-filler bonds. It was determined using Eq. (4):

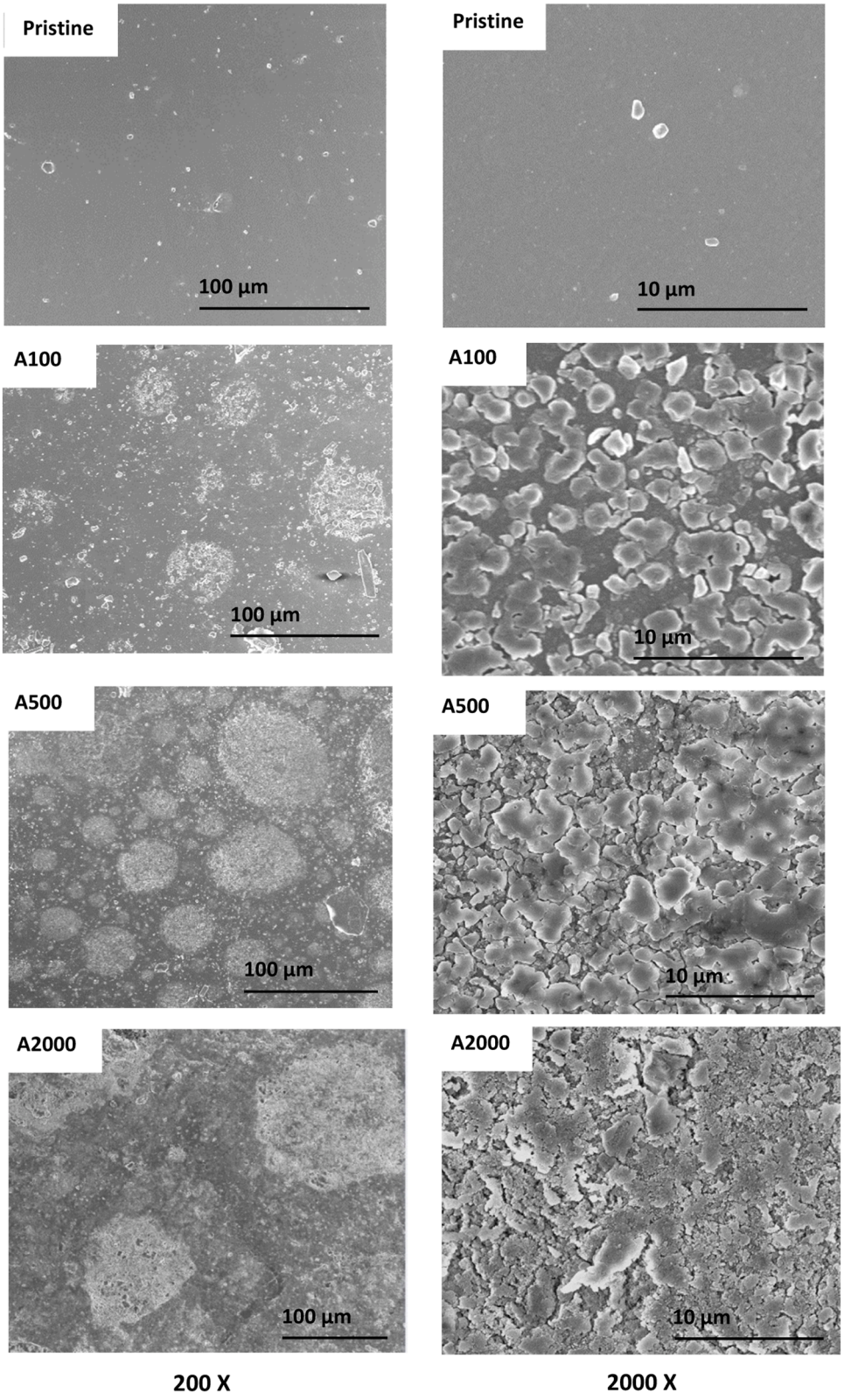

Fig. 2. SEM micrographs of pristine and aged samples, at magnifications of 200X and 2000X.

$$\Delta Vr\ (\%) = \left(1 - \frac{SR^M}{SR^A}\right) * 100 \quad (4)$$

Where and are the swelling ratios determined from protocol 1 and protocol 2, respectively.

It was decided not to calculate the molar mass between crosslinks using Flory Rehner theory to avoid the uncertainty in the proper quantitative values, relative to the interaction parameter between polymer and solvent [21,22] and how it may evolve during ageing. For each determination, the results of three specimens were averaged.

2.2.6. NMR spectroscopy

Solid-state ^{29}Si NMR analyses were conducted on a Bruker Avance-400 MHz NMR spectrometer operating at ^{29}Si resonance frequency of 79.5 MHz. About 80 mg of specimen, cut from the 2 mm diameter silicone rubber sheets, were placed in a zirconium dioxide rotor of 4 mm outer diameter and spun at a Magic Angle Spinning rate of 8 kHz in a commercial Bruker Double Channel probe. The experiments were performed with Cross Polarization (CP) technique [23] using a ramped ^{1}H pulse starting at 100 % power and decreasing until 50 % during the contact time (5ms) to circumvent Hartmann-Hahn mismatches [24]. To improve the resolution, a dipolar decoupling GT8 pulse sequence [25] was applied during the acquisition time. The spectra were obtained with an accumulation of 14 000 scans using a delay of 2,5 s for 10 h experimental time for each specimen, which allowed a good signal-to-noise ratio. The ^{29}Si chemical shifts were referenced to tetramethylsilane.

3. Results

3.1. SEM observations

SEM micrographs of the surface of pristine and aged silicone rubber samples, at magnifications of 200X and 2000X, are presented in Fig. 2. Before ageing, pristine sample shows a uniform and smooth surface morphology. After 100 ageing cycles, small circular spots of inhomogeneous diameter appear on the sample surface. At higher magnification, those spots seem to be cracked areas of the material surface. As the number of ageing cycles increases, the number and diameter of these spots become bigger, and cracks become wider and deeper. The aged samples surface become chalky, and the roughness and chalkiness can be felt even by touching the surface. These cracks show up the extent of silicone rubber degradation upon hydrothermal ageing. These observations are quite similar to the surface state after natural and artificial ageing of silicone composite insulators as reported by Zeng et al. [26]. The chalking observed after natural ageing is particularly associated with the emergence of silica particles on the surface due to the degradation of the polymer matrix.

3.2. Weight loss and TGA

Fig. 3 depicts the weight loss (%) versus number of ageing cycles. The weight loss increases linearly with the number of ageing cycles and reached 21.9 % after 2000 ageing cycles. To determine whether the weight loss origins from the polymer, the fillers, or both, TGA were conducted on pristine and aged samples. Fig. 4 shows TGA curves of pristine and aged samples. The residue increases with the number of ageing cycles. Under nitrogen, silicone rubber decomposes entirely at temperature above 400 °C by random chain scission mechanism, forming volatile cyclic oligomers [27]. In these conditions, the residue is attributed to the weight content of silica in silica filled silicone rubber [28]. As displayed in Fig. 4, the increase of residue with the number of ageing cycles suggests therefore that the weight loss measured during ageing mainly results from the polymer and not from the fillers. To verify this hypothesis, the silica weight content was calculated from TGA and weight loss data, assuming the weight loss resulted only from the polymer (Table 1).

As evinced in Table 1, the weight content of silica in pristine and aged samples calculated from weight loss measurements data is consistent with that calculated from TGA data, confirming that the weight loss concerns mainly the polymer. The variation in results that are seen for 2000 cycles can be explained by the fact that the weight loss measurements results are an average weight loss on the entire sample, while the TGA results depend on where the specimen was cut, center or near sample edge and thus could be affected by the inhomogeneity of the ageing on the samples surface, that increases as the number of ageing cycles increases [29].

Table 2 shows the temperature at 5 % weight loss from TGA curves for pristine and aged samples. The temperature at which degradation begins increases with ageing, with the greatest increase during the first 100 cycles.

3.3. Infrared spectroscopy

Fig. 5 shows FTIR spectra of pristine and aged samples surface. The band at 790 cm^{-1} is characteristic of CH_3 rocking and Si-C asymmetric stretching. Bands at 1010 cm^{-1} and 1060 cm^{-1} are attributed to Si-O-Si symmetric and asymmetric stretching, respectively [30]. Band at 1259 cm^{-1} is characteristic of symmetric -CH_3 bend [30]. Amorphous silica fillers (including fumed silica [31]) are characterized by a broad shoulder at 1220 cm^{-1} and a band at 1060 cm^{-1} [32]. Bands at 2904 cm^{-1} and 2960 cm^{-1} are attributed to asymmetric and symmetric stretching of CH_3 in Si-CH_3, respectively [30]. A decrease in bands intensity over the entire spectrum is observed after 2000 ageing cycles, as compared to other samples. This is probably due to the irregularities on

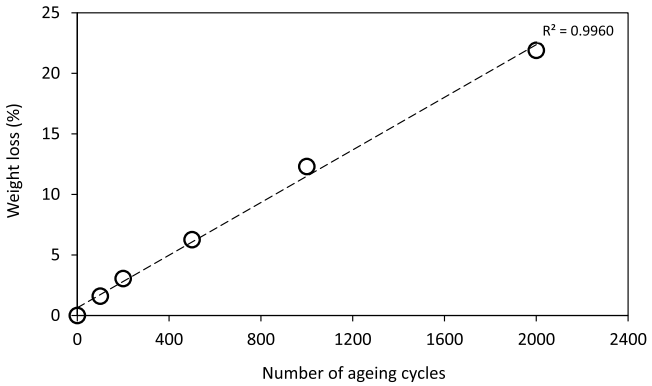

Fig. 3. Weight loss (from Eq. 1) as a function of the number of ageing cycles.

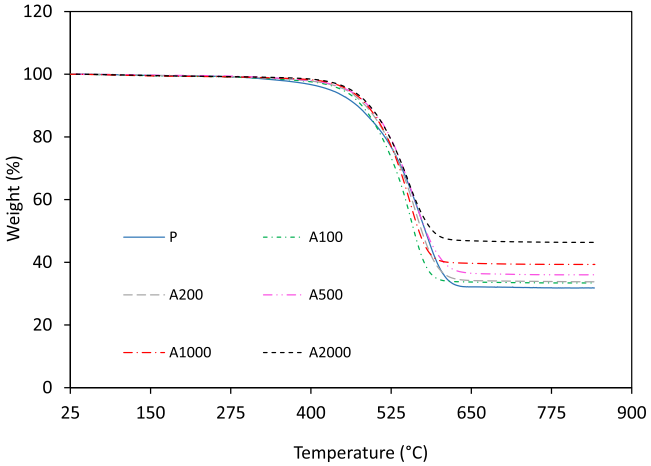

Fig. 4. TGA curves of pristine and aged samples.

Table 1
Silica content (Wt%) of pristine and aged samples calculated from weight loss measurements and TGA.

Sample	Weight loss (%)	Silica content (Wt%) (weight loss data)[a]	Silica content (Wt%) (TGA data)[b]
P	0	32	32 ± 0.3
A100	1.6	32.7	32,9 ± 0.4
A200	3.0	33	33 ± 0.4
A500	6.3	34	35 ± 0.9
A1000	12.3	37	38 ± 1.5
A2000	21.9	41	44 ± 2.8

[a] The error of weight loss measurements is below 1 %.
[b] The standard deviation was calculated from 3 measurements.

Table 2
Temperature at 5 % weight loss ($T_{d5\ \%}$) of pristine and aged samples.

Sample	$T_{d5\ \%}$ (°C)
P	432 ± 3
A100	449 ± 2
A200	456 ± 2
A500	459 ± 1
A1000	462 ± 1
A2000	466 ± 0

the sample surface (as shown in SEM micrographs). This irregular surface leads to poor quality contact with the ATR diamond crystal, which limits the amount of material analyzed.

As shown in Fig. 5, notable changes in the absorbance of the main bands of the filled silicone rubber occurred after hydrothermal ageing. On one hand, the band at 1259 cm^{-1} decreased monotonously with ageing cycles number, suggesting a loss of polymer fragments. On the other hand, the absorbance of silica at 1220 cm^{-1} and 1060 cm^{-1} increased monotonously with ageing cycles number indicating an increase of silica content at the samples surface, undoubtedly because of the polymer loss. The broad band at 3400 cm^{-1} may refer to the stretching vibrations of the silanol groups of silica [33] or end chain silanol groups as well as water molecules bound to the silica [34]. It is therefore very complex to assess the origin of the changes in the intensity of this band, especially since the width of the band is likely to evolve during ageing due to modifications in hydrogen bond interactions of these groups. It is important to note that the lower absorbance at 3400 cm^{-1} after 2000 cycles is only due to a poorer contact with the ATR crystal (vide supra). The ratio of the absorbance at 3400 cm^{-1} to the absorbance of $SiCH_3$ at 2960 cm^{-1}, showed a continuous increase in this ratio during successive cycling (Fig. S4). While the increase in the absorption intensity at 3400 cm^{-1} can be associated with the formation of end chain silanol formed by hydrolysis of the polymer, the increase observed for the subsequent cycles is more difficult to interpret. However, it is very likely that the increase beyond 100 ageing cycles is mainly due to the increase in silica content in the material, with silica contributing more to the absorption at 3400 cm^{-1} (surface silanol groups and bound water) compared to the polymer matrix.

The absorbance ratio at 1220 cm^{-1} to the absorbance at 1259 cm^{-1}

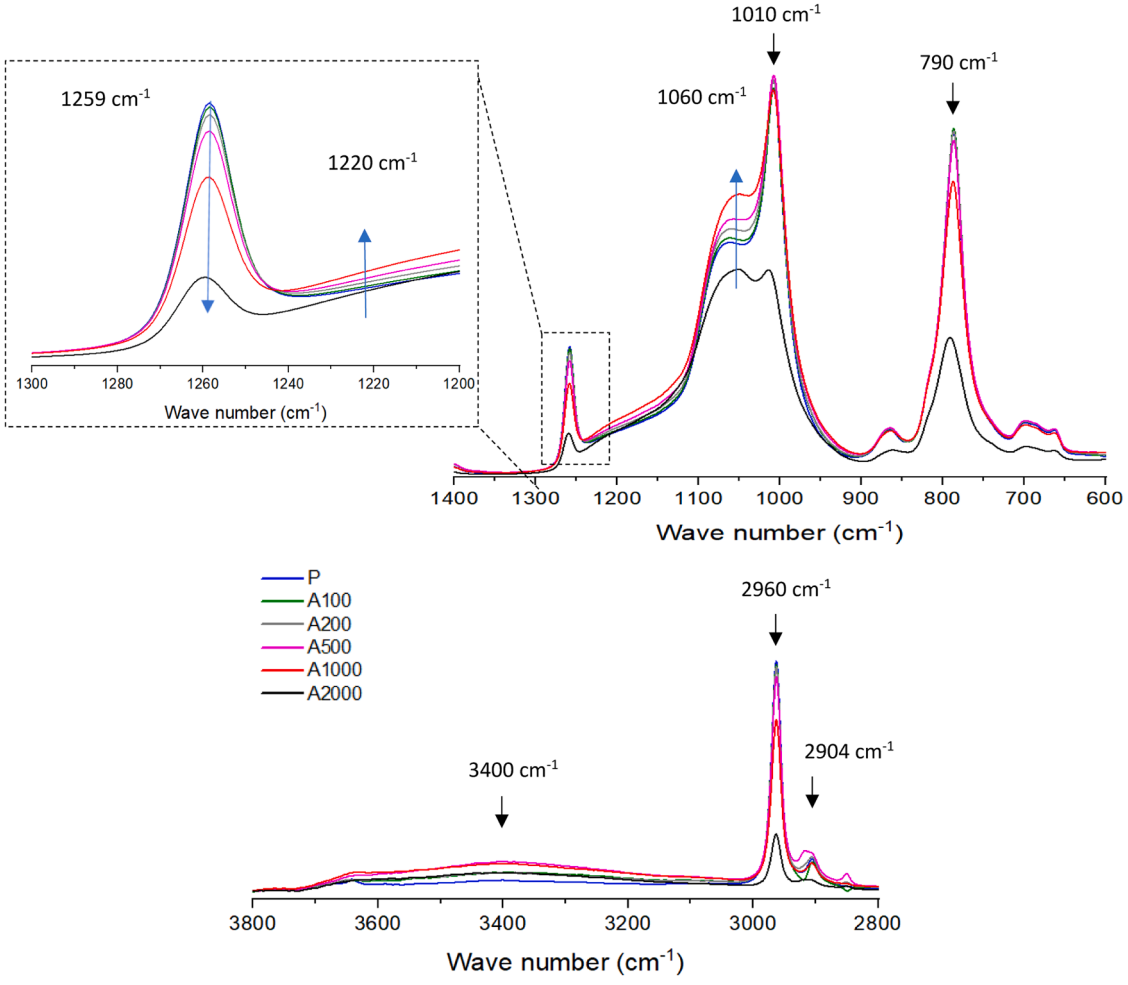

Fig. 5. FTIR spectra of pristine and aged silicone rubber samples.

was calculated and plotted as a function of the number of ageing cycles, as shown in Fig. 6. The ratio was calculated from FTIR spectra at the samples surface and at ~ 1 mm from the surface (after cutting the sheets of 2 mm thickness in the bulk).

As depicted in Fig. 6, the absorbance ratio (H 1220 / H 1259) increases as the number of ageing cycles increases, confirming an increase of silica content at the samples surface. The increase of the absorbance ratio (H 1220 / H 1259) at the samples surface is much higher than that in the bulk. The difference widens from 200 cycles upwards. This indicates an ageing gradient in the material thickness, more prominent as the number of ageing cycles increases.

3.4. Swelling

Fig. 7 shows the evolution of swelling ratio, in methylcyclohexane and in methylcyclohexane under ammonia atmosphere as function of the number of ageing cycles.

The swelling ratio of silicone rubber in methylcyclohexane increases up to 500 ageing cycles and then seems to reach a relatively stable value beyond that. The overall increase of swelling ratio is very slight, as it increases from 362 % before ageing to 372 % after 2000 ageing cycles which represents an increase of 2.8 %. Polymer-filler interactions between silicone chains and silica surface contribute to the total crosslink density through physical network. Thus, the ammonia modified swelling protocol is of great interest to determine the contribution of physical interactions, specifically hydrogen bonds between silica and siloxane chains, to the total crosslink density. The procedure was first introduced by Polmanteer and Lenz [35] as the ammonia is believed to cleave hydrogen bonds between polymer and fillers. As expected, the swelling ratio in methylcyclohexane under ammonia is higher than that in methylcyclohexane because of the rupture of physical polymer-filler attachments by ammonia (Fig. 7). In methylcyclohexane under ammonia, the swelling ratio decreases up to 200 ageing cycles, then increases from 200 cycles to 500 ageing cycles and reaches a plateau from 1000 cycles to 2000 cycles. To quantify the contribution of physical polymer-filler interactions to the total crosslink density and its evolution upon hydrothermal ageing, the network chain decrement was calculated. The evolution of versus number of ageing cycles is presented in Fig. 8.

Network chain decrement decreases in the early stages of ageing until 200 cycles and then increases slightly from 500 cycles to 2000 cycles. However, after 2000 ageing cycles, remains lower than before ageing. The changes of during ageing suggests that major modifications occurred at polymer-filler interfaces.

Fig. 9 shows the evolution of extractable fraction in methylcyclohexane and in methylcyclohexane under ammonia versus number of ageing cycles.

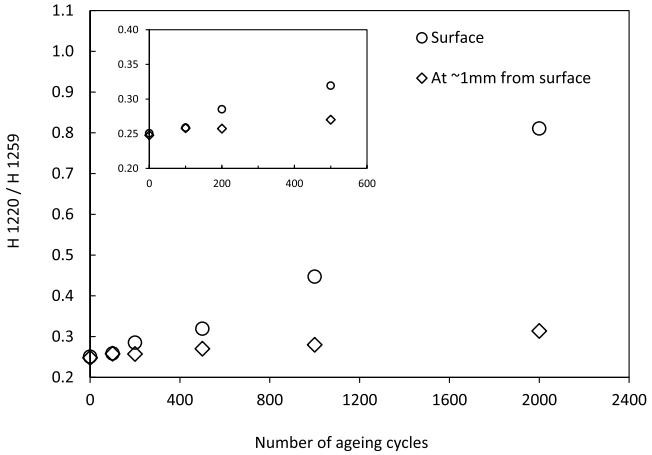

Fig. 6. Absorbance ratio (H1220/H1259) versus number of ageing cycles.

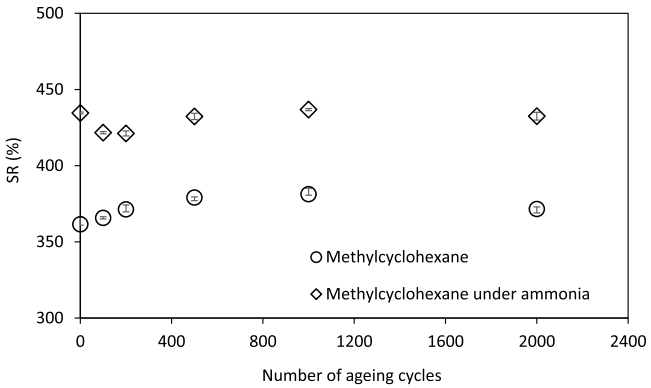

Fig. 7. Swelling ratio (SR) versus number of ageing cycles.

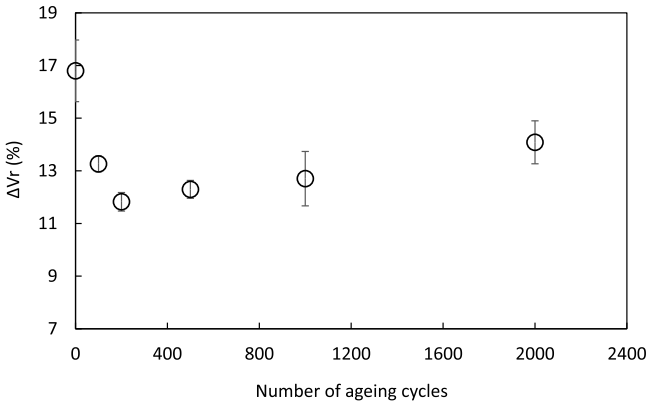

Fig. 8. Network chain decrement (ΔVr) versus number of ageing cycles.

Regardless of the swelling protocol, the extractable fraction decreases with the number of ageing cycles and is nearly null after 2000 cycles. Before ageing, the extractable fraction could be attributed to the residual free chains present in the network (e.g. processing aid and free VMQ chains), which can then be extracted in the solvent during swelling [22]. The extractable fraction is slightly higher under ammonia atmosphere, indicating that around 20 % of the free chains in the pristine sample are in physical interaction with silica fillers. The proportion of free chains interacting with silica decreases over the first 200 cycles and then fluctuates with no clear trend.

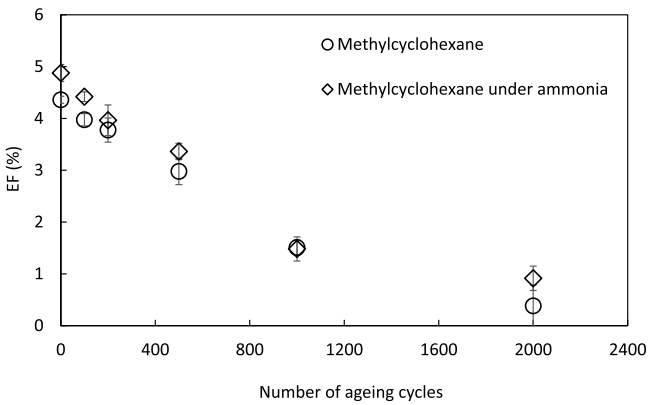

Fig. 9. Extractable fraction (EF) versus number of ageing cycles.

3.5. NMR spectroscopy

^{29}Si CP-MAS NMR analysis were conducted on pristine and aged samples to assess the modifications that occur at polymer-filler interfaces during the hydrothermal ageing. The ^{29}Si CP-MAS spectra, in the region of −130 to 30 ppm are presented in Fig. 10.

The spectra exhibit a narrow signal at ~ −22 ppm, characteristic of D dimethylsiloxy units in long PDMS chains. An additional broad signal at a lower field is observed in the region of D units at about −18 ppm. The origin of this signal, which is shifted to a lower field compared to the dimethylsiloxy units of long PDMS chains, will be discussed later. The two components in the Q region at ~ −100 ppm and ~ −110 ppm are characteristic respectively of single silanol groups Q^3 and siloxane units Q^4 of silica fillers [36,37]. To better understand the changes at silica surface during ageing, the peaks Q^3 and Q^4 were deconvoluted. The deconvolution was performed using OriginLab Pro software and Gaussian – Lorentz cross deconvolution was chosen and processed without any baseline correction (Fig. 11). The chi square values of all deconvoluted spectra were higher than 0.99. The ratio of the peak area Q^4 to the peak area Q^3 named Q^4/Q^3 ratio, was calculated from the fit.

As shown in Fig. 12, the Q^4/Q^3 ratio increases sharply during the first 100 cycles, then more slowly for subsequent cycles, finally reaching a more or less constant value beyond 500 cycles. The increase of Q^4/Q^3 ratio corresponds to an increasing number of siloxane groups in the detriment of single silanol groups.

4. Discussion

4.1. Chemical degradation of the polymer network

As evidenced by weight loss (Fig. 3), TGA (Fig. 4 and Table 1), and FTIR (Fig. 5) data, the weight loss that occurred during hydrothermal ageing comes undoubtedly from the loss of the polymer and not the fillers. Given the ageing conditions, the loss of polymer fragments occurs mainly during the vacuum phases. The degradation mechanism therefore induces the formation of volatile species. Pioneering works in the 1950s and 1960s demonstrated that, while silicone rubber is thermally stable up to temperatures generally over 350 °C, it decomposes in the presence of water at much lower temperatures [38,39]. In particular, it has been shown that hydrolysis reactions occur in the 120 °C-275 °C range in a humid atmosphere [38]. Hydrolysis of siloxane bonds in the polysiloxane backbone results in the formation of OH-terminated siloxane chains that have lower thermal stability than trimethylsilyl ended PDMS [40]. According to thermal degradation studies, it has been well established that OH-terminated PDMS chains depolymerize via Si-O bond scission in a stepwise fashion from chain ends to yield cyclic oligomeric siloxanes [40]. The formation of small volatile cycles by backbiting reaction, such as D_3 and D_4, and their evacuation during the vacuum phases, thus explains the significant weight loss observed throughout the successive cycles. Given that backbiting generally occurs at higher temperatures than that of the actual ageing procedure (134 °C) [11,41], the presence of a catalytic species in the compound of our study is likely. As mentioned in the introduction, the presence of certain impurities is known to significantly lower the degradation temperature of silicone rubber materials, so much so that the depolymerization process can occur at temperatures as low as 100 °C [16,42]. Scheme 1 illustrates the primary degradation mechanisms of the polymer network: hydrolysis and backbiting reaction.

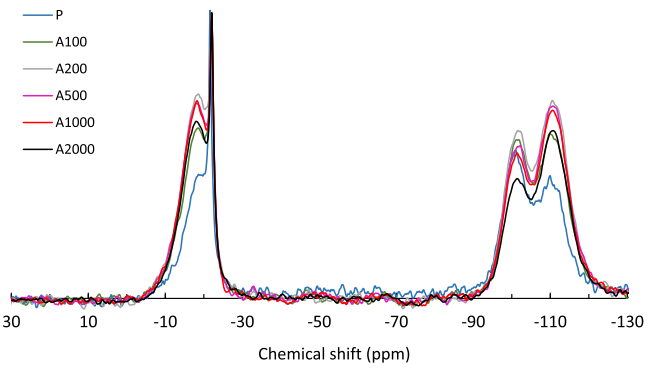

Fig. 10. ^{29}Si CP MAS spectra of pristine and aged samples in the 30 - −130 ppm region.

^{29}Si NMR spectra revealed that the relative intensity of silanol end groups M^{OH} at ~ −12 ppm [43] compared to that of dimethylsiloxy D units at ~ −22 ppm increases after 100 ageing cycles. This highlights the hydrolysis of the dimethylsiloxane chains. The increase in IR absorption at 3400 cm^{-1} during the first 100 cycles (Fig. S4) is primarily attributed to the hydrolysis of the dimethylsiloxane chains, which predominates over the condensation reactions of the silanols during the initial cycles. The M^{OH} signal appears to change little beyond 100 ageing cycles which suggests that an equilibrium between hydrolysis and recombination reactions has been established. It should be noted that this is not a true equilibrium. Hydrolysis reactions occur during the steam exposure phase while condensation reactions between silanol groups occur more likely during the vacuum phases, as the hydrolysis-condensation equilibrium is displaced by the evacuation of water molecules. Since the concentration of silanol end groups in polymer chains rapidly becomes constant during successive cycles, the rate of formation of volatile cycles varies little, which explains the continuous and linear weight loss over time (Fig. 3). The reversibility of hydrolysis-condensation reactions is also reflected in swelling results. The swelling ratio in methylcyclohexane increases only during the first 500 ageing cycles, while little change is observed for subsequent cycles (Fig. 7). The relative stability in swelling over 500 cycles, does not mean however, that the network topology remains unchanged. The stabilization of swelling ratio is due to compensation effects between scission and recombination reactions, but the network topology undoubtedly evolves throughout the ageing process. Furthermore, the high stability of the Si-C bond to hydrolysis reactions is reflected in the absence of T signals in the −40 - −80 ppm region (Fig. 10). This also evinces that the ageing conditions are not severe enough to observe homolytic cleavage of the Si-C bonds [41]. Other changes observed in the ^{29}Si NMR spectra and swelling measurements suggest that significant modifications at the polymer-filler interfaces occur, primarily during the first few hundred ageing cycles. This will be discussed in detail in Section 4.2.

TGA results showed an increase in the onset degradation temperature ($T_{d5\ \%}$) during the ageing cycles (Table 2). The increase in $T_{d5\ \%}$ appears to have little correlation with the increase of silica content, in line with previously reported results [44]. In fact, the shift of $T_{d5\ \%}$ was the most significant after 100 cycles while in parallel, the weight loss was only about 1.8 %, which confirms that this shift cannot be solely related to the enhanced silica content upon the ageing. Fig. 9 shows that the amount of extractable chains decreases with the number of ageing cycles, becoming almost negligible after the highest number of ageing cycles. This indicates that few free chains are formed during the ageing, and that the extractable chains are mainly derived from the pristine sample (sol fraction related to network imperfections and processing aid). The low volatility of these siloxane free chains means that they cannot be evacuated during vacuum phases [45]. Thus, the reduction in the amount of extractable chains is probably due to the decrease in the molar mass of free chains following backbiting reactions, but also to their anchoring on silica surface via a siloxane bond (vide infra). The shift in onset temperature observed after ageing therefore appears to be controlled by the decrease in the amount of free OH-terminated chains in the aged samples.

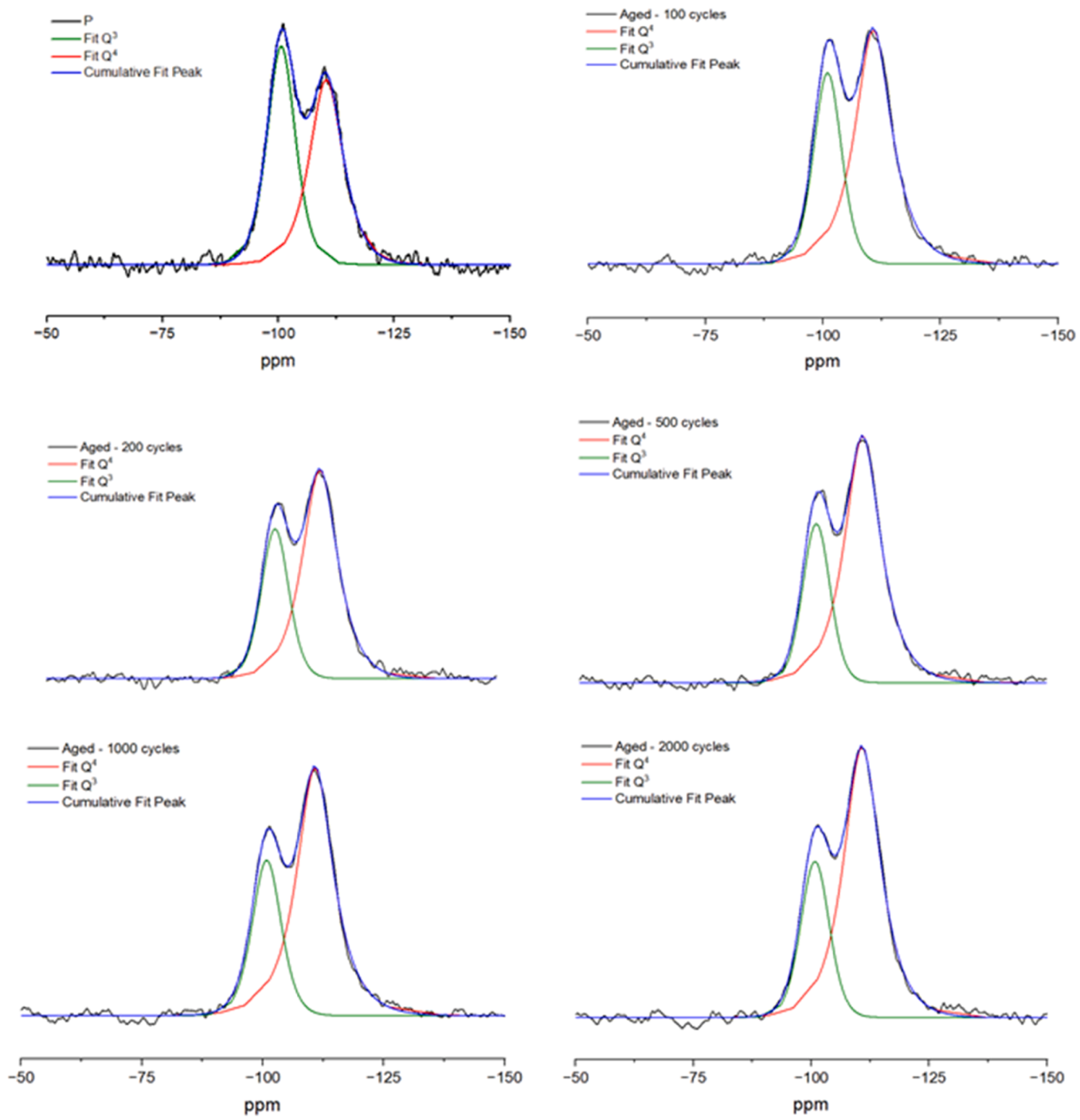

Fig. 11. ^{29}Si CP-MAS spectra of pristine and aged samples in the −50—150 ppm region.

4.2. *Rearrangements at polymer-filler interfaces*

Swelling experiments results (Figs. 7 and 8) and ^{29}Si solid NMR data (Figs. 10 and 11) highlight the rearrangements that occurred at polymer-filler interfaces during ageing. Until 200 cycles, the decrease of reflects a lowering in the contribution of hydrogen interactions between silica and siloxane chains to the total crosslink density, which is consistent with the increase of Q^4/Q^3 ratio. Examining the D region of ^{29}Si NMR spectra is also highly instructive. The resonance observed at ∼ −22 ppm is characteristic of dimethylsiloxy units such as those found in long PDMS chains. The assignment of the broad signal at ∼ −18 ppm in the D region of NMR spectra is more complicated but it may be attributed to D units close to Q units [46]. It has been reported by Babonneau et al. [47] that an enhanced response of this peak was observed for ^{29}Si CP-MAS sequence compared to ^{29}Si MAS. The enhanced cross-polarization response was related to a difference in the mobility of methyl groups which may affect the average of the dipolar interactions between the protons and Si nuclei [47]. Therefore the broad component at about −18 ppm was attributed to D units close to Q units in TEOS/PDMS gels [47]. As silica content increases with ageing, a continuous increase in the intensity of the −18 ppm signal relative to that of the signal at∼ −22 ppm might be expected. This is not the case, as there is a significant increase over the first 200 ageing cycles, followed by little changes over the subsequent cycles (with even a tendency to decrease slightly for the highest number of cycles). These changes cannot be explained simply by an increase in the silica fraction, and therefore reflect an evolution in the

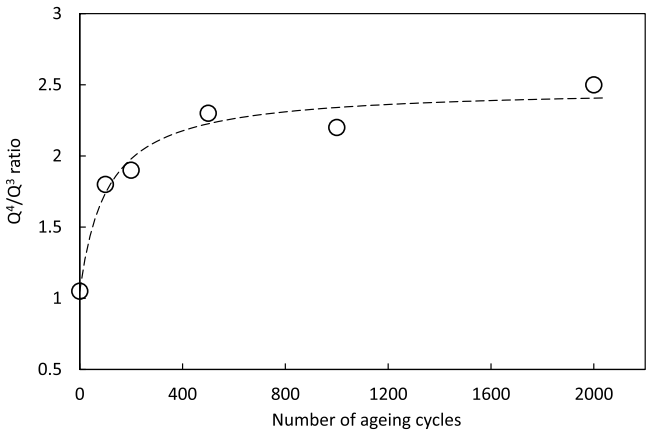

Fig. 12. Q^4/Q^3 ratio versus number of ageing cycles (the dash line is a guide to the eye).

structure of the polymer-filler interphase during ageing. The D signal associated to dimethylsiloxy units at the vicinity of silica surface and with constrained mobility, increases sharply over the first 200 cycles, while silica content has changed very little in parallel. This result, combined with the large increase in the silica condensation state over the same period (as revealed by the increase of Q^4/Q^3 ratio), suggests the formation of highly constrained oligodimethylsiloxane chains on silica surface participating to the crosslinked network. In addition to the formation of new covalent bonds between the silica and silicone networks, the creation of small loops consisting of a few dimethylsiloxy units may contribute to an increased proportion of dimethylsiloxy units with low mobility. Previous research has demonstrated the significant role of physisorbed water in reactions between polysiloxanes and silica [48]. The Lewis acidic centers, which were most likely created by water adsorbed onto silica surface defects initiate the hydrolysis of the adsorbed siloxanes chains, and then silanols were coupled to the surface to generate grafted siloxanes, according to the hypothesized reaction mechanism [48]. The formation of highly constrained oligodimethylsiloxane chains on silica surface participating to the crosslinked network is consistent with the decrease of swelling under ammonia observed in the first 100 cycles (Fig. 7). Unlike physical crosslinks, chemical crosslinks remain active under ammonia, helping to reduce swelling. When swelling is carried out in methylcyclohexane (with no ammonia), both physical and chemical crosslinks are active. Consequently, the evolution of the polymer network topology contributes more to the observed swelling evolution.

Fig. 9 shows that the proportion of free chains (processing aid and residual free chains in the network) in physical interaction with silica decreases sharply over the first 200 cycles. In addition to backbiting, the condensation of free chains with the silica surface therefore undoubtedly contributes to the decrease in the extractable fraction during the first 200 ageing cycles.

5. Conclusion

In this research, the ageing of a silica filled silicone rubber formulation was studied using a combination of physico-chemical analyses. We focused first on the degradation of the polymer network, then on the evolution of polymer-filler interactions. Hydrolytic scission of siloxane bonds in the polymer and reverse recombination reactions occur during steam exposure and vacuum phases, respectively. The ageing cycle induces the continuous formation of volatile cycles through backbiting reaction. In parallel, solvent extraction results showed that few free siloxane chains are formed during ageing. The oligomeric cycles are evacuated during vacuum phases, which lead to an increase in the silica content of the material. As a result, the structure of the silicone rubber is affected by both the dry steam and vacuum phases of the prion cycle.

In addition to changes in the topology of the polymer network, a significant change in the silica-polymer interfacial region has been demonstrated. Condensation reactions between the silanol groups at silica surface and polymer chains occur, particularly during the first ageing cycles. These reactions are accompanied by an increase in the concentration of low mobility dimethylsiloxane units. The strong affinity of silica for water molecules is assumed to be at the origin of polymer-filler condensation process, since it causes extensive hydrolysis of dimethylsiloxane units at the vicinity of silica surface and subsequent grafting by connecting silanol groups.

In the present paper, we have identified the main modes of degradation of a silicone rubber subjected to pressure steam phases that alternated with vacuum phases. A forthcoming paper will be dedicated to the influence of these degradation modes on the mechanical properties of the material.

CRediT authorship contribution statement

Manar Ramram: Writing – original draft, Investigation. **Lénaïk Belec:** Writing – review & editing, Supervision. **Jean-François Chailan:** Writing – review & editing, Supervision. **François Perseil Rouillard:** Writing – review & editing, Supervision. **François-Xavier Perrin:** Writing – review & editing, Supervision, Conceptualization.

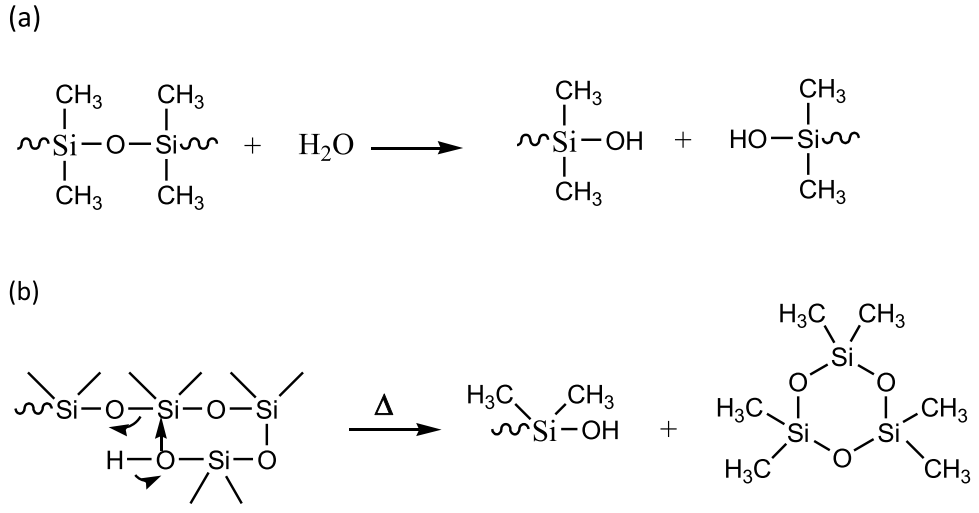

Scheme 1. H. ydrolysis (a) and depolymerization by unzipping reaction (b) of PDMS chains.

Declaration of competing interest

The authors declare that they have no known competing financial interests or personal relationships that could have appeared to influence the work reported in this paper.

Acknowledgements

Ageing experiments were conducted in Maestral, a joint laboratory of CEA/DES/ISEC and TECHNETICS GROUP.

The authors would like to thank Dr. Alain Pouchelon (OTECI) and Mr. Michel Berger for the valuable discussions, Dr. Fabio Ziarelli for solid NMR analyses, Mr. Nans Durey for his contribution to the ageing experiments and Mr. Jérôme Guillot for the preparation of the samples.

Supplementary materials

Supplementary material associated with this article can be found, in the online version, at doi:10.1016/j.polymdegradstab.2025.111332.

Data availability

The authors do not have permission to share data.

References

[1] S.J. Clarson, Silicones and Silicone-Modified Materials: A Concise Overview, in: Synthesis and Properties of Silicones and Silicone-Modified Materials, American Chemical Society, 2004, pp. 1–10.
[2] M. Andriot, J. DeGroot, R. Meeks, E. Gerlach, M. Jungk, A. Wolf, D. Corning, S. Cray, T. Easton, A. Mountney, S. Leadley, S.H. Chao, Silic. Ind. Applic. (2009).
[3] S.C. Shit, P. Shah, A Rev. Silic. Rubber, Natl. Acad. Sci. Lett. 36 (2013) 355–365, https://doi.org/10.1007/s40009-013-0150-2.
[4] P.R. Dvornic, Thermal Properties of Polysiloxanes, in: Silicon-Containing Polymers: The Science and Technology of Their Synthesis and Applications, Springer, Netherlands, 2000, pp. 185–212, https://doi.org/10.1007/978-94-011-3939-7_7.
[5] F. de Buyl, Silicone sealants and structural adhesives, Int. J. Adhes. Adhes. 21 (2001) 411–422, https://doi.org/10.1016/S0143-7496(01)00018-5.
[6] G. Wypych, Fillers - origin, chemical composition, properties, and morphology. Handbook of Fillers, 4th Edition, ChemTec Publishing, 2016, pp. 13–266, https://doi.org/10.1016/B978-1-895198-91-1.50004-X.
[7] H. Barthel, L. Rösch, J. Weis, Fumed silica - production, properties, and applications. Organosilicon Chemistry Set, John Wiley & Sons, Ltd, 2005, pp. 761–778, https://doi.org/10.1002/9783527620777.ch91a.
[8] A. Ansarifar, B. Lim, Reinforcement of silicone rubber with precipitated amorphous white silica nanofiller – Effect of silica aggregates on the rubber properties, J. Rubber Res. 9 (2006) 140–158.
[9] S.E. Shim, A.I. Isayev, Rheology and structure of precipitated silica and poly (dimethyl siloxane) system, Rheol. Acta 43 (2004) 127–136, https://doi.org/10.1007/s00397-003-0327-6.
[10] B. Rupasinghe, J. Furgal, Degradation of silicone-based materials as a driving force for recyclability, Polym. Int. 71 (2022) 521–531, https://doi.org/10.1002/pi.6340.
[11] S. Kole, S.K. Srivastava, D.K. Tripathy, A.K. Bhowmick, Accelerated hydrothermal weathering of silicone rubber, EPDM, and their blends, J. Appl. Polym. Sci. 54 (1994) 1329–1337, https://doi.org/10.1002/app.1994.070540915.
[12] S. Rubinsztajn, M. Cypryk, J. Chojnowski, Behavior of oligo(dimethylsiloxanols) in the presence of protic acids in an acid-base inert solvent. Kinetics of the competition of disproportionation, ester formation, and condensation, Macromolecules. 26 (1993) 5389–5395, https://doi.org/10.1021/ma00072a015.
[13] I.A. Metkin, V.P. Mileshkevich, V.B. Pavlova, Hydrolytic stability of polyorganosiloxanes as a function of their structure, Polym. Sci. U.S.S.R 23 (1981) 606–616, https://doi.org/10.1016/0032-3950(81)90006-X.
[14] F.M. Lewis, The science and technology of silicone rubber, Rubber Chem. Techn. 35 (1962) 1222–1275, https://doi.org/10.5254/1.3539992.
[15] A. Labouriau, T. Robison, L. Meincke, D. Wrobleski, D. Taylor, J. Gill, Ageing mechanisms in RTV polysiloxane foams, Polym. Degrad. Stab. 121 (2015) 60–68, https://doi.org/10.1016/j.polymdegradstab.2015.08.013.
[16] N. Grassie, I.G. Macfarlane, The thermal degradation of polysiloxanes—I. Poly (dimethylsiloxane), Eur. Polym. J. 14 (1978) 875–884, https://doi.org/10.1016/0014-3057(78)90084-8.
[17] J.F. Masson, I. Lopez–Carreon, J. Wu, O. Obukohwo, P. Collins, M. Riahinezhad, E. Esmizadeh, Degradation and service-life prediction of silicone rubber in a highly alkaline environment simulating concrete, Eng. Fail. Anal. 138 (2022) 1–15, https://doi.org/10.1016/j.engfailanal.2022.106305.
[18] G. Ducom, B. Laubie, A. Ohannessian, C. Chottier, P. Germain, V. Chatain, Hydrolysis of polydimethylsiloxane fluids in controlled aqueous solutions, Water. Sci. Technol. 68 (2013) 813–820, https://doi.org/10.2166/wst.2013.308.
[19] P. Vondráček, M. Schätz, NH3-modified swelling of silica-filled silicone rubber, J. Appl. Polym. Sci. 23 (1979) 2681–2694, https://doi.org/10.1002/app.1979.070230913.
[20] A.M. Stricher, R.G. Rinaldi, C. Barrès, F. Ganachaud, L. Chazeau, How I met your elastomers: from network topology to mechanical behaviours of conventional silicone materials, RSC. Adv. 5 (2015) 53713–53725, https://doi.org/10.1039/C5RA06965C.
[21] A. Pouchelon, C. George, P. Menez, The swelling behaviour of siloxane elastomers in relation to their microscopic structure, Macromol. Symp. 171 (2001) 233–242, https://doi.org/10.1002/1521-3900(200106)171:1<233::AID-MASY233>3.0.CO;2-5.
[22] W. Chassé, M. Lang, J.U. Sommer, K. Saalwächter, Cross-link density estimation of PDMS networks with precise consideration of networks defects, Macromolecules. 45 (2012) 899–912, https://doi.org/10.1021/ma202030z.
[23] J. Schaefer, E.O. Stejskal, Carbon-13 nuclear magnetic resonance of polymers spinning at the magic angle, J. Am. Chem. Soc. 98 (1976) 1031–1032, https://doi.org/10.1021/ja00420a036.
[24] O.B. Peersen, X.L. Wu, I. Kustanovich, S.O. Smith, Variable-amplitude cross-polarization MAS NMR, J. Magn. Reson., Ser.A 104 (1993) 334–339, https://doi.org/10.1006/jmra.1993.1231.
[25] G. Gerbaud, F. Ziarelli, S. Caldarelli, Increasing the robustness of heteronuclear decoupling in magic-angle sample spinning solid-state NMR, Chem. Phys. Lett. 377 (2003) 1–5, https://doi.org/10.1016/S0009-2614(03)01056-X.
[26] S. Zeng, X. Zhao, W. Li, Y. Peng, Y. Liu, X. Yan, G. Zhang, Performance comparison and lifespan assessment of naturally and artificially chalked silicone rubber for composite insulators, Polym. Degrad. Stab. 232 (2025) 111139, https://doi.org/10.1016/j.polymdegradstab.2024.111139.
[27] T.S. Radhakrishnan, New method for evaluation of kinetic parameters and mechanism of degradation from pyrolysis–GC studies: thermal degradation of polydimethylsiloxanes, J. Appl. Polym. Sci. 73 (1999) 441–450, https://doi.org/10.1002/(SICI)1097-4628(19990718)73:3<441::AID-APP16>3.0.CO;2-J.
[28] E. Delebecq, S. Hamdani - Devarennes, J. Raeke, J.M. Cuesta, F. Ganachaud, High residue contents indebted by platinum and silica synergistic action during the pyrolysis of silicone formulations, ACS. Appl. Mater. Interfaces. 3 (2011) 869–880, https://doi.org/10.1021/am101216y.
[29] D. Chen, C. Huang, X. Hu, Preparation and characterization of novel polydimethylsiloxane composites used POSS as cross-linker and fumed silica as reinforcing filler, Polym. Compos. 34 (2013) 1041–1050, https://doi.org/10.1002/pc.22511.
[30] J.J.H. Lancastre, N. Fernandes, F.M.A. Margaça, I.M. Miranda Salvado, L. M. Ferreira, A.N. Falcão, M.H. Casimiro, Study of PDMS conformation in PDMS-based hybrid materials prepared by gamma irradiation, radiation, Phys. Chem. 81 (2012) 1336–1340, https://doi.org/10.1016/j.radphyschem.2012.02.016.
[31] A. Grard, L. Belec, F.X. Perrin, Characterization and evaluation of primer formulations for bonding silicone rubber to metal, Prog. Org. Coat. 140 (2020) 1–11, https://doi.org/10.1016/j.porgcoat.2019.105513.
[32] P. Launer, B. Arkles, Infrared analysis of organosilicon compounds, in: Silicon Compd. Silanes Silicones, 3rd Ed., 2013: pp. 175–178.
[33] Y. Song, J. Yu, D. Dai, L. Song, N. Jiang, Effect of silica particles modified by in-situ and ex-situ methods on the reinforcement of silicone rubber, Mater. Des. 64 (2014) 687–693, https://doi.org/10.1016/j.matdes.2014.08.051.
[34] F. Sundfors, T. Lindfors, L. Höfler, R. Bereczki, R.E. Gyurcsányi, FTIR-ATR study of water uptake and diffusion through ion-selective membranes based on poly (acrylates) and Silicone rubber, Anal. Chem. 81 (2009) 5925–5934, https://doi.org/10.1021/ac900727w.
[35] K.E. Polmanteer, C.W. Lentz, Reinforcement studies—Effect of silica structure on properties and crosslink density, Rubber Chem. Techn. 48 (1975) 795–809, https://doi.org/10.5254/1.3539687.
[36] C.C. Liu, G.E. Maciel, The fumed silica surface: a study by NMR, J. Am. Chem. Soc. 118 (1996) 5103–5119, https://doi.org/10.1021/ja954120w.
[37] H. Zou, S. Wu, J. Shen, Polymer/silica nanocomposites: preparation, characterization, properties, and applications, Chem. Rev. 108 (2008) 3893–3957, https://doi.org/10.1021/cr068035q.
[38] D.K. Thomas, Network scission processes in peroxide cured methylvinyl silicone rubber, Polymer. 7 (1966) 99–105, https://doi.org/10.1016/S0032-3861(66)80005-8.
[39] R.C. Osthoff, A.M. Bueche, W.T. Grubb, Chemical stress-relaxation of polydimethylsiloxane Elastomers1, J. Am. Chem. Soc. 76 (1954) 4659–4663, https://doi.org/10.1021/ja01647a052.
[40] N. Grassie, I.G. Macfarlane, The thermal degradation of polysiloxanes—I. Poly (dimethylsiloxane), Eur. Polym. J. 14 (1978) 875–884, https://doi.org/10.1016/0014-3057(78)90084-8.
[41] G. Camino, S.M. Lomakin, M. Lageard, Thermal polydimethylsiloxane degradation. Part 2. The degradation mechanisms, Polymer. 43 (2002) 2011–2015, https://doi.org/10.1016/S0032-3861(01)00785-6.
[42] M. Kučera, J. Láníková, Thermal stability of polydimethylsiloxane. I. Deactivation of basic active centers, J. Poly. Sci. 54 (1961) 375–384, https://doi.org/10.1002/pol.1961.1205416009.
[43] R.K. Harris, M.L. Robins, 29Si nuclear magnetic resonance studies of oligomeric and polymeric siloxanes: 4. Chemical shift effects of end-groups, Polymer. 19 (1978) 1123–1132, https://doi.org/10.1016/0032-3861(78)90057-5.
[44] E. Delebecq, S. Hamdani-Devarennes, J. Raeke, J.M. Lopez Cuesta, F. Ganachaud, High residue contents indebted by platinum and silica synergistic action during the pyrolysis of silicone formulations, ACS. Appl. Mater. Interfaces. 3 (2011) 869–880, https://doi.org/10.1021/am101216y.

[45] Y.D. Lei, F. Wania, D. Mathers, Temperature-dependent vapor pressure of selected cyclic and linear polydimethylsiloxane oligomers, J. Chem. Eng. Data 55 (2010) 5868–5873, https://doi.org/10.1021/je100835n.
[46] V.M. Litvinov, H. Barthel, J. Wets, The structure of a PDMS layer grafted onto a silica surface studied by means of DSC and solid-State NMR. Organosilicon Chemistry Set, John Wiley & Sons, Ltd, 2005, pp. 715–735, https://doi.org/10.1002/9783527620777.ch113d.
[47] F. Babonneau, L. Bois, J. Livage, S. Dire, Structural investigation of sol-gel-derived hybrid siloxane-oxide materials using 29Si mas-nmr spectroscopy, MRS Online Proceed. Libr. 286 (1992) 289–294, https://doi.org/10.1557/PROC-286-289.
[48] G. Graffius, F. Bernardoni, A.Y. Fadeev, Covalent functionalization of silica surface using “inert” poly(dimethylsiloxanes), Langmuir. 30 (2014) 14797–14807, https://doi.org/10.1021/la5031763.